Cover letter: 2. FMT **Topics: 2. Fluid Mechanics and Thermodynamics**

Numerical analysis of the effects of free-stream thermo-chemical state on the test model flow field in high-enthalpy tunnel

Ming Zeng [1,2], Jun Liu[2], Zhen-bin Lin[1], Zhang-hua Qu[2]

(1. Laboratory of High-Temperature Gas Dynamics, Institute of Mechanics, Chinese Academy of Sciences, Beijing 10080, China; 2. College of Aerospace and Material Engineering, National University of Defense Technology, Changsha 410073, China)

Abstract: The effects of the free-stream thermo-chemical state on the test model flow field in the high-enthalpy tunnel are studied numerically. The properties of the free-stream, which is in thermo-chemical non-equilibrium, are determined by calculating the nozzle flow field. A free-stream with total enthalpy equal to the real one in the tunnel while in thermo-chemical equilibrium is constructed artificially to simulate the natural atmosphere condition. The flow fields over the test models (blunt cone and Apollo command capsule model) under both the non-equilibrium and the virtual equilibrium free-stream conditions are calculated. By comparing the properties including pressure, temperature, species concentration and radiation distributions of these two types of flow fields, the effects of the non-equilibrium state of the free-stream in the high-enthalpy shock tunnel are analyzed.

Key words: high-enthalpy shock tunnel, numerical simulation, hypersonic flow, thermo-chemical non-equilibrium, high-temperature air radiation

1 INTRODUCTION

High-enthalpy shock tunnel is an important type of impulse facility to evaluate the high-temperature real-gas effects on the fluid-mechanical behavior of hypersonic flows. By analyzing Navier-Stokes equation for real-gas flow and the chemical kinetics equations, Zhang[1] gives the principles which must be followed in the ground simulation of high-temperature non-equilibrium flow. It is pointed out that fully simulation of the hypersonic flight is impossible, only part of the characteristics of the hypersonic flow can be simulated in the ground test facility. This is just the case for the high-enthalpy shock tunnel. In the analysis[1] the vibrational temperature of the gas is assumed in equilibrium with the translational/rotational temperature, and the species concentration of the free-stream is assumed the same as the quite natural atmosphere, namely, in thermo-chemical equilibrium.

In the reservoir of the high-enthalpy shock tunnel, the test gas is at a high temperature, and therefore, is in a significantly vibrationally excited, dissociated, or ionized state. During the cooling process occurring in the nozzle, vibrational de-excitation and recombination processes move the gas state toward that of the natural atmosphere. However, these processes require time to complete, and since the gas temperature changes so rapidly in the nozzle, the gas fails to reach the thermo-chemical equilibrium condition of the natural atmosphere at the nozzle exit[2]. This phenomenon is known as thermo-chemical freezing, and it may be a new cause of

uncertainties in the ground simulation of hypersonic flight.

Many numerical studies of the hypersonic non-equilibrium flow have been done[3]. However, most of them are concerning the flow field over the vehicles flying at hypersonic speed in atmosphere at high altitude, there are few incorporate calculations of the nozzle flow filed and the test model flow field in the high-enthalpy tunnel, and there are even fewer numerical analyses of the effects of the free-stream thermo-chemical state on the test model flow field, which is important to the extrapolation of experimental data to the flight condition.

How the test model flow field being affected by the non-equilibrium state of the free-stream is studied numerically in this paper, with the aim to supply quantitative references to the validity evaluation of the ground simulation. Since non-equilibrium scale effects exist in the nozzle flow filed of high-enthalpy tunnel[4], the free-stream thermo-chemical state may be different for tunnels with different scales. The investigation in this paper aims at the detonation driven high-enthalpy shock tunnel JF-10, which was built at Institute of Mechanics, Chinese Academy of Sciences, Beijing.

The properties of the free-stream, being in thermo-chemical non-equilibrium, are determined by calculating the hypersonic nozzle flow field. To simulate the thermo-chemical condition of the natural atmosphere, a free-stream is constructed artificially by modifying some properties of the above non-equilibrium free-stream: setting the air composition as that of the natural atmosphere condition and the vibrational temperature equal to the translational temperature, then converting the vibrational and chemical energy of the gas to kinetic energy, namely, increasing the gas velocity. In this way, the artificial free-stream is in thermo-chemical equilibrium, and the total enthalpy of the artificial ‘equilibrium free stream’ is equal to the real non-equilibrium one.

The flow fields over the test models (spherically blunted cone and Apollo command capsule scale model) under both the non-equilibrium and the virtual equilibrium free-stream conditions are calculated, the effects of the free-stream thermo-chemical state on the test model flow field properties, including pressure, temperature, species concentration and radiation distributions are analyzed by comparing these two types of flow fields.

In the present numerical simulation, the nozzle flow field and the test model flow field in the test section is calculated sequentially instead of the incorporate calculations of the whole high-enthalpy tunnel flow field. The core flow properties in the test section can be determined in this way while the complex computation of the flow near the wall of the test section is avoided.

2 GOVERNING EQUATIONS AND CALCULATION METHOD

2.1 Thermo-chemical model

Both thermal and chemical non-equilibrium assumption is taken in the present study. One vibrational temperature T_v is taken for all diatomic molecules, and the translational temperature T is assumed in equilibrium with the rotational temperature. Millikan and White’s vibrational relaxation formula corrected by Park[5] is used to compute the vibrational relaxation time. In the nozzle flow field calculation, the high temperature air consists of 7 species: N_2, O_2, N, O, NO, NO^+, e^-; in the test model flow field calculation, 11-species model is used (N_2^+, O_2^+, N^+, O^+ also considered) for computation of the radiation properties, because N_2^+ may be an important

radiation species. The chemical kinetics are based on Gupta's 32-reaction model[6], and different rate-controlling temperatures are employed for different reactions to reflect the coupling of the vibrational and chemical processes[7]. For example, the rate-controlling temperatures are $T^{1/2}T_v^{1/2}$ for dissociating reactions while are T_v for the electron-impact ionizing reactions.

2.2 Governing equations

In a cylindrical coordinate system, the axisymmetric thermo-chemical non-equilibrium Navier-Stokes equations are the following:

$$\frac{\partial \boldsymbol{U}}{\partial t}+\frac{\partial \boldsymbol{E}}{\partial x}+\frac{\partial \boldsymbol{F}}{\partial r}+\boldsymbol{H}=\frac{1}{Re}\left(\frac{\partial \boldsymbol{F}_v}{\partial x}+\frac{\partial \boldsymbol{G}_v}{\partial r}+\boldsymbol{H}_v\right)+\boldsymbol{W} \tag{1}$$

The vector of conservative quantities is given by

$$\boldsymbol{U}=\left(\rho C_1,\rho C_2,\cdots,\rho C_{ns},\rho u,\rho v,E,E_v\right)^T \tag{2}$$

the vector $\boldsymbol{W}$ is the vibrational and chemical source terms

$$\boldsymbol{W}=\left(\dot{w}_1,\dot{w}_2,\cdots,\dot{w}_{ns},0,0,0,S_v\right)^T \tag{3}$$

where C_i and $\dot{w}_i$ are the mass fraction and chemical source term of species i respectively, E_v is the vibrational energy and S_v is the vibrational source term. The detailed description of other vectors is in Ref.[8].

The three-dimensional thermo-chemical non-equilibrium Navier-Stokes equations in an orthogonal coordinate system are:

$$\frac{\partial \boldsymbol{U}}{\partial t}+\frac{\partial \boldsymbol{E}}{\partial x}+\frac{\partial \boldsymbol{F}}{\partial y}+\frac{\partial \boldsymbol{G}}{\partial z}=\frac{1}{Re}\left(\frac{\partial \boldsymbol{E}_v}{\partial x}+\frac{\partial \boldsymbol{F}_v}{\partial y}+\frac{\partial \boldsymbol{G}_v}{\partial z}\right)+\boldsymbol{W} \tag{4}$$

The vectors $\boldsymbol{U}$ and $\boldsymbol{W}$ are similar to Eq.(2) and Eq.(3), the detailed meanings of other vectors can be found in Ref.[8].

The axisymmetric N-S equations (1) are solved for nozzle flow field, the axisymmetric N-S equations (1) or the 3-dimensional N-S equations (4) are solved for test model flow field.

2.3 Radiation model

With the knowledge of the density, temperature and species concentration distribution, the radiation characteristics of the flow field is computed. The quasi-steady-state (QSS) approximation is employed to figure out the populations of the different excited states. Using the line-by-line model[9], the spectral absorption and emission coefficients at any specific spatial point can be computed from electronic transitions of diatomic molecules and atoms according to the local conditions. Emission and absorption coefficients are both in the radiation transfer equation under thermal non-equilibrium condition[10]. Considering that the shock layer is much thinner than the nose radius and the gradients in the normal direction are much larger than those in the tangent direction, the tangent-slab model is employed in solving the radiation transfer equation.

2.4 Computational method

The N-S equations coupled with the vibrational and chemical kinetics equations are solved to obtain the steady state solution of the flow field. A fully implicit finite difference approach is used in the calculation, all inviscid terms are discretized with AUSMPW+[11] scheme and the viscous terms are discretized with center difference scheme, the implicit parts of the differential equations are disposed in two steps with LU-SGS approach[12].

3 Calculation of the nozzle flow field

The reservoir temperature and pressure are 7920K and 19.6MPa respectively. The conical nozzle is 2m long, the half-angle is 7.1-deg, the throat and exit diameters are 11mm and 500 mm respectively. Considering that the flow continues expanding after the nozzle exit, the calculated nozzle has an exit area ratio of 2838.

The mesh distribution must be quite stretched near the throat and the wall to capture correctly the flow gradients around the throat region and in the boundary layer. A mesh system of 118×101 points is used with $\Delta x_{\min}=5.93\times10^{-4}$m located at the throat section, $\Delta y_{\min}=5.29\times10^{-7}$m at the wall of the throat section, and $\Delta y_{\min}=2.82\times10^{-4}$m at the wall of the exit section. For the boundary conditions of the computational domain, a detailed description is given in a previous paper[13].

7-species and 2-temperature thermo-chemical model is used in the calculation of the nozzle flow field. The core flow properties at the nozzle exit are listed in Table 1, they are taken as the free-stream properties in the test section. As this free-stream consists of 7 species and the vibrational temperature differs from the translational temperature, it is named 7S2T free-stream. The propertis of the virtual free-stream that simulates the natural atmosphere are determined as follows: the translational temperature, pressure, density are set equal to those of 7S2T free-stream (see Table 1), but the air composition is set the same as that of the natural atmosphere, the vibrational temperature is set equal to the translational temperature, then the velocity is increased by converting the vibrational and chemical energy of the gas to kinetic energy. In this way, the total enthalpy of the virtual equilibrium free-stream is equal to the real non-equilibrium one in the tunnel. The virtual free stream consists of only 2 species and its vibrational temperature is the same as its translational temperature, so it is named 2S1T free-stream, its velocity is listed in Table 1.

Table 1 Free-stream properties in the test section

Pressure, temperature, velocity, etc.		Species mass fraction C_i	
pressure p [Pa]	95	N_2	0.745
translational temperature T [K]	436	O_2	0.065
vibrational temperature T_v [K]	3210	O	0.146
density ρ [kg/m^3]	0.00067	NO	0.044
velocity U_{7S2T} [m/s]	4990	N	0.84×10^{-8}
velocity U_{2S1T} [m/s]	**5530**	NO^+	0.54×10^{-6}

4 RESULTS AND DISCUSSION

In this section the properties of the flow fields over the test models under the non-equilibrium 7S2T and the equilibrium 2S1T free-stream conditions are compared to examine the effects of the free-stream thermo-chemical state.

Two blunt cone with similar half-angle but different ratio of spherical nose to base radius (50% and 10%) are selected in the present analysis, and they are named Cone-A and Cone-B respectively. The axisymmetric flow field and radiation field of a 0.1 Apollo command capsule scale model is also investigated.

4.1 The axisymmetric flow field of Cone-A

Cone-A is a spherically blunted cone. The half-angle is 8.2-deg, the spherical nose radius is 0.035m and the total length of the cone is 0.276m. Its nose shock wave is strong and the gas is significantly dissociated or ionized in the shock layer, so 11-species and 2-temperature thermo-chemical model is used in calculating the axisymmetric flow field. The effects of free-stream non-equilibrium on temperature distributions, species distributions and on heat transfer are investigated. The full catalytic wall condition is assumed and the wall temperature is assumed equal to 300K. A mesh system of 71×61 points is used and the mesh distribution is stretched near the wall.

Fig. 1 is the pressure contour of the flow-field under 7S2T free-stream condition. The pressure contour under 2S1T free-stream condition is similar, but the shock layer is thinner. Fig. 2 gives the density distributions along the stagnation line. It can be seen that under the 7S2T free-stream condition the average density ratio between the shock layer and the free-stream is smaller than that under 2S1T condition, and this is the cause of the increase in the thickness of the shock layer.

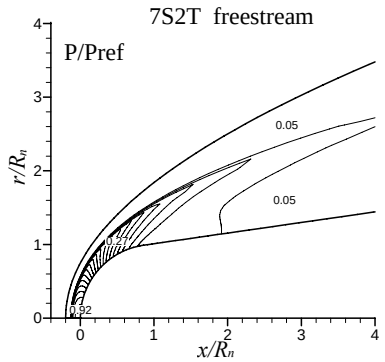

Fig. 1 Pressure contour of Cone-A in 7S2T free-stream

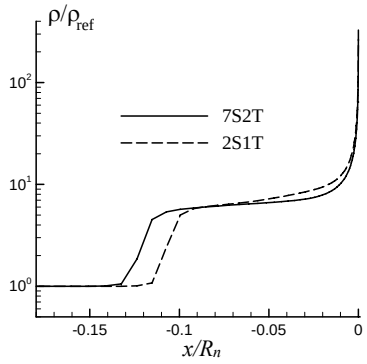

Fig. 2 Density distributions along stagnation line of Cone-A

The temperature distributions along the stagnation line is shown in Fig. 3. The translational temperature increase quickly after the shock wave while there is a great lag in the increase in vibrational temperature, almost the whole shock layer is in thermal non-equilibrium state. The peak value of translational temperature under 7S2T free-stream condition is much lower than that under 2S1T condition.

The mass fraction distributions of N and NO^+ along the stagnation line are given in Fig. 4 and Fig. 5 respectively. There is also a lag between the increase of temperature and the chemical

reaction process. The lag is more significant under 2S1T free-stream condition, so in most region of the shock layer the dissociation and ionization are less under 2S1T condition despite the higher translational temperature than that under 7S2T condition.

The distributions of heat transfer *St* number along the cone wall are depicted in Fig. 6. Because the region of dissociation and ionization around the model is wider under 7S2T free-stream condition, there are more atoms and ions combined at the cool catalytic wall and therefore the heat released to the wall is more than that under 2S1T condition.

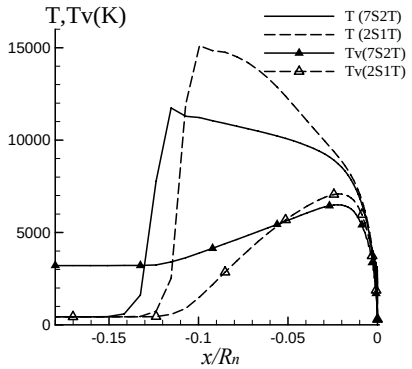

Fig. 3 Temperature distributions along stagnation line of Cone-A

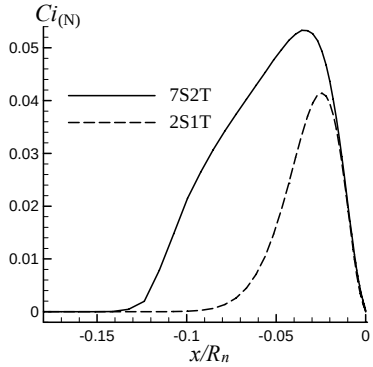

Fig. 4 Mass fraction distributions of N along stagnation line of Cone-A

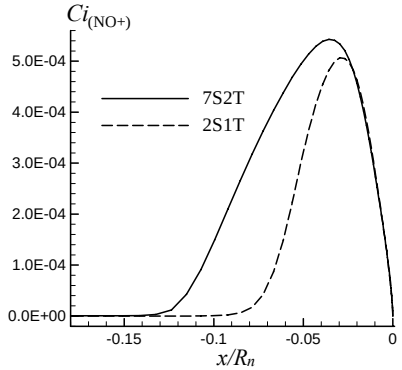

Fig. 5 Mass fraction distributions of NO＋ along stagnation line of Cone-A

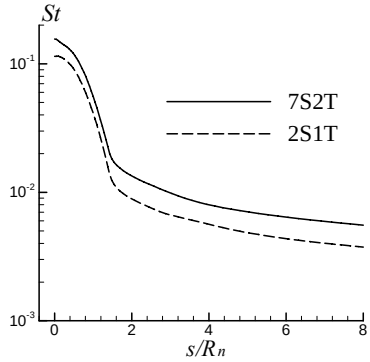

Fig. 6 St numbers of Cone-A

4.2 The 3-dimensional flow field of Cone-B

The spherical nose radius of Cone-B is 0.00508m, The half-angle is 10-deg and the total length of the cone is 0.2639m. 7-species and 2-temperature model is used in calculating its 3-dimensional flow filed, the effects of the free-stream non-equilibrium on the aerodynamic force and moment are examined. The full catalytic wall condition is assumed and the wall temperature is assumed equal to 300K. A mesh system of 83×61×19 points is used and the mesh distribution is stretched near the wall.

The aerodynamic force and pitching moment coefficients of Cone-B at the attack angles of 15 and 10-deg for the two free-stream conditions are listed in Table 2, the nose-up pitching moment is defined positive. The lift coefficients under 7S2T condition are a little higher than those under 2S1T condition, the lift coefficient is 2% higher at attack angle of 15-deg and 2.5%

higher at attack angle of 10-deg. The drag coefficients under 7S2T condition are also higher in some sort than those under 2S1T condition, but only 0.3% higher at 15-deg and 0.7% higher at 10-deg. As for the pitching moment, there is a increase of 1.5% at attack angle of 15-deg and 2.3% at 10-deg in nose-down pitching moment under 7S2T free-stream condition.

Table 2 Aerodynamic coefficients of Cone-B

Angle of attack	15-deg		10-deg	
free-stream thermo-chemical state	7S2T	2S1T	7S2T	2S1T
lift coefficient C_L	0.310	0.304	0.204	0.199
drag coefficient C_D	0.214	0.213	0.142	0.141
pitching moment coefficient $C_{m,O}$	-0.203	-0.200	-0.131	-0.128

The influence of the real gas effects on aerodynamic characteristics is well known. The heat absorption by chemical reactions behind a shock wave causes a decrease in the effective γ, and thereby increases the average density ratio between the shock layer and the free-stream. To satisfy the mass continuity condition, the shock layer thickness decreases inversely with the density ratio. This lowers the angle of the shock wave formed over an inclined surface, which leads to a lower lift and a nose-up pitching moment[2]. But as can be seen in Cone-A case (Fig. 2) and in Cone-B case (Table 2), the non-equilibrium condition of the free-stream affects the flow field inversely in some sort, that is, the free-stream non-equilibrium in the high-enthalpy shock tunnel discount its capacity of reflecting real-gas effects on aerodynamic characteristics to some extent.

4.3 The axisymmetric flow field of Apollo model

The axisymmetric flow field of a 0.1 Apollo command capsule scale model is also investigated. The spherical nose radius of the model is 0.4595m, the diameter of the maximum cross section is 0.395m and the total length is 0.3522m. Considering the gas in the high-temperature shock layer of the capsule model is highly dissociated and ionized and some species may emit radiation, 11-species and 2-temperature model is used in calculating the flow field, and the effects of the free-stream non-equilibrium on the species distributions, electron density and radiation properties are analyzed. A mesh system of 105×77 points is used and the mesh distribution is stretched near the wall.

Fig. 7 is the pressure contour of the flow-field under 7S2T free-stream condition. Under 2S1T condition the pressure contour is similar except that the shock layer is thinner.

The temperature distributions along the stagnation line is shown in Fig. 8. The increase in the shock layer thickness resulted from the non-equilibrium of the free-stream is more evident in the Apollo scale model case than that in Cone-A (Fig. 3). The peak value of translational temperature under 7S2T free-stream condition is much lower than that under 2S1T condition. Owing to the large nose radius, the region of thermal non-equilibrium after the shock is relatively small, and in the region of thermal equilibrium, about three-fourths of the shock-layer, the temperature distributions under 7S2T and 2S1T conditions are similar.

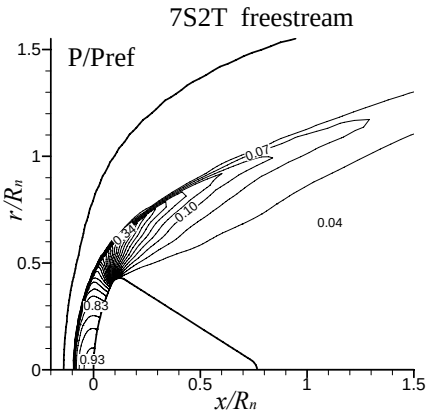

Fig. 7 Pressure contour of Apollo model in 7S2T free-stream

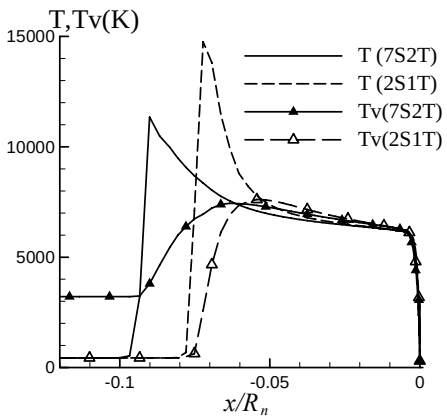

Fig. 8 Temperature distributions along stagnation line of Apollo model

The mass fraction distributions of N and N_2^+ along the stagnation line are given in Fig. 9 and Fig. 10. The lag between the increase of temperature and the chemical reaction process is not so severe under the 7S2T free-stream condition, so after the shock wave the mass fractions of NO, atoms and ions reach their peak values earlier under 7S2T condition. The region of high temperature (see Fig. 8) and highly dissociation around the model is wider under 7S2T condition. Because of the Apollo model's bigger scale, the degree of the non-equilibrium of the chemical reactions in the shock-layer is not so significant as Cone-A case, the peak values of most species are close under 7S2T and 2S1T conditions.

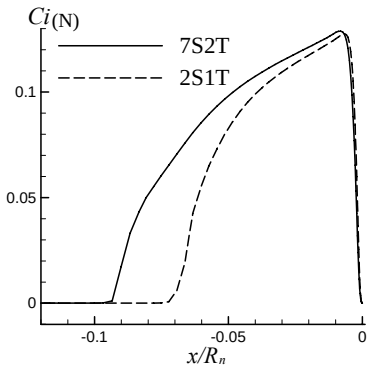

Fig. 9 Mass fraction distributions of N along stagnation line of Apollo model

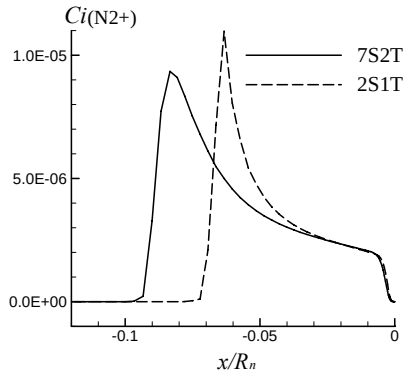

Fig. 10 Mass fraction distributions of N_2^+ along stagnation line of Apollo model

With the knowledge of the temperature, density and species concentration distributions in the flow field, the emission and absorption coefficients at 80000 wavelength points in 800A~6000A are computed along the stagnation line, and the radiation transfer equation is solved to obtain the spectral radiation intensity I_λ to the stagnation in the normal direction. I_λ at every adjacent 40 points are averaged, and the averaged values at 2000 wavelength points in 800A~6000A are shown in Fig. 11. There are densely distributed spectral lines for λ<1500A, which originate from the atomic bound-bound transitions, for λ>1500A, the spectra that originate mainly from the molecules radiation are almost continuous. The orders and spectral distribution characteristics of I_λ are similar under both free-stream conditions, but the value under 7S2T condition is a little lower. Although the region of high temperature and highly

dissociation or ionization around the model is wider under 7S2T condition, the position of peak values is farther and therefore the radiation attenuation is more, in addition, the average density in the shock layer is about 20% lower under 7S2T condition, so I_λ is still a little lower under 7S2T free-stream condition.

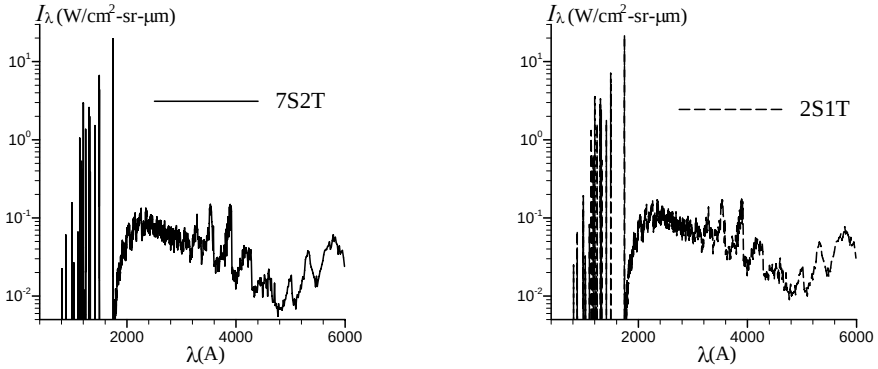

Fig. 11 Spectral radiation intensity I_λ to stagnation of Apollo model in normal direction

5 CONCLUSION

High-enthalpy shock tunnel can generate the test gas with high velocity for simulating the high-temperature real-gas effects. But in such a tunnel, the freezing phenomenon takes place during the gas expansion process in the nozzle, and the free-stream in the test section is in thermo-chemical non-equilibrium state, which is different from the natural atmosphere. With the purpose of analyzing the effects of the free stream thermo-chemical condition, a free-stream with total enthalpy equal to the real one in the high-enthalpy shock tunnel while in equilibrium is constructed artificially. The comparisons between the flow field properties under the non-equilibrium free-stream condition and those under the virtual equilibrium free-stream condition show that:

(1) The non-equilibrium free-stream contains some atoms and ions. On the one hand, this limits the extent of more dissociation and ionization in the shock-layer and thereby limits the decrease ratio of the effective γ, so the average density in the shock layer is lower, which leads to the increase in the thickness of shock layer. On the other hand, a free-stream containing vibrationally excited or dissociated or ionized species produces reaction rates faster than a equilibrium free-stream, therefore, the concentration of atoms and ions attain their peak values earlier, this also broadens the region of high temperature and the region of dissociation and ionization.

(2) The well known influence of the real gas effects on aerodynamic force and moment results from the increase in the average density ratio between the shock layer and the free-stream, however, the non-equilibrium state of the free-stream discount this increase. Accordingly, in the ground simulation of aerodynamic force and moment, it is necessary to evaluate the produced density ratio and then evaluate that to what degree the true real-gas effects are realized.

(3) Due to the broadening of the region of dissociation and ionization around the model, there are more atoms and ions combined at the catalytic wall, which leads to higher wall heat transfer rates in the non-equilibrium the free-stream.

(4) The non-equilibrium state of the free-stream causes a increase in the thickness of the

shock layer and changes the species distributions, therefore the electric and radiation properties of the flow field is affected in some sort.

(5) The thermo-chemical state of the free-stream in the high-enthalpy shock tunnel will influence the model test results to some extent. For different aspects of the aerodynamic performance, for models with different shapes or different scales, the effects of the free-stream thermo-chemical state may be different. Through detailed numerical analysis, one may obtain helpful advice on the test strategy for ground simulation as well as on the extrapolation of tunnel data to real flight.

REFERENCES

[1] Zhang H-X. The Similarity Law for Real Gas Flow. Acta Aerodynamic Sinica. 1990, 8(1)：1～8 (in Chinese).

[2] Park C. Evaluation of Real-Gas Phenomena in High-Enthalpy Impulse Test Facilities: A Review. Journal of Thermophysics and Heat Transfer, 1997, 11(1)：10～18.

[3] Gnoffo P A, Weilmuenster K J, Hamilton II H H, Olynick D R, Venkatapathy E. Computational Aerothermodynamic Design Issues for Hypersonic Vehicles. Journal of Spacecraft & Rockets. 1999，36(1)：21～43.

[4] Zeng M, Lin Z-B, Feng H-T, Qu Z-H. Numerical Analysis of Non-equilibrium Scale Effects in Hypersonic Nozzle. Journal of Propulsion Technology. 2005, 26(1)：38～41 (in Chinese).

[5] Park C. Problems of Rate Chemistry in Flight Regime of Aeroassisted Orbital Transfer Vehicles. Progress in Aeronautics and Astronautics, 1985, 96 (Thermal Design of Aeroassisted Orbital Transfer Vehicles, edited by Nelson H F, AIAA, New York)：511～537.

[6] Gupta R N, Yos J M, Thompson R A, et al. A Review of Reaction Rates and Thermodynamic and Transport Properties for an 11-species Air Model for Chemical and Thermal Non-equilibrium Calculations to 30000K. NASA RP 1232，1990.

[7] Park C. Nonequilibrium Hypersonic Aerothermodynamics. John Wiley & Sons. 1990.

[8] Liu J. Experimental and Numerical Research on Thermochemical Nonequilibrium Flow with Radiation Phenomenon. PHD Thesis. Changsha, China: National University of Defense Technology. 2004 (in Chinese).

[9] Arnold J, Cooper D, Park C. Line-by-Line Transport Calculations for Jupiter Entry Probes. AIAA 79-1082, 1979.

[10] Huang H. Numerical Study of Non-equilibrium Flow Field Coupled with Radiation. PHD Thesis. Changsha, China: National University of Defense Technology. 2000 (in Chinese).

[11] Kim K H, Kim C, Rho O H. Accurate Computations of Hypersonic Flows Using AUSMPW+ Scheme and Shock-Aligned Grid Technique. AIAA 98-2442, 1998.

[12] Stoll P, Gerlinger P, Brüggemann D. Domain Decomposition for An Implicit LU-SGS Scheme Using Overlapping Grids. AIAA 97-0770, 1997.

[13] Zeng M, Feng H-T, Lin Z-B, Qu Z-H. Analysis of Viscous Effects on Measurement of Free-Stream Pressure in High-Enthalpy Shock Tunnel Test Section. Journal of Experiments in Fluid Mechanics. 2006, 20(1)：1～4 (in Chinese).